

Optimizing Carbonation Hardening for Lightweight Concrete

Olexander Gara, Anatoliy Gara, Andrii Kolesnykov, Khrystyna Moskalova*

Abstract: This study investigates the accelerated carbonation hardening (ACH) of lightweight aggregate concrete. It evaluates the effects of binder content, ground limestone, lightweight aggregates, plasticizers, carbonation pressure, and duration on compressive strength at 1 hour, 28 days, and 180 days. Statistical models and optimization using desirability functions were employed to identify optimal recipe and technological parameters. ACH enhances concrete strength and promotes sustainable carbon sequestration, providing an alternative to conventional curing methods.

Keywords: accelerated carbonation; lightweight concrete; optimization; recipe factors; response surface

1 INTRODUCTION

Accelerated carbonation hardening (ACH) has become an effective approach to enhancing the mechanical properties and environmental performance of concrete. In contrast to traditional methods like steam curing, which demand significant energy and resources, ACH provides a sustainable alternative by utilizing CO₂ to improve strength and durability while capturing atmospheric carbon dioxide [1-3]. The process accelerates carbonation reactions in cement-based materials, forming calcium carbonate, which densifies the concrete matrix and improves its properties [4-5]. This method is particularly advantageous for applications requiring rapid curing, such as bridges and high-rise buildings in challenging environments, where durability and efficiency are critical [6].

Optimizing ACH involves controlling factors such as binder composition, CO₂ pressure, and curing time. This study investigates these parameters using statistical methods to enhance the effectiveness of ACH, ensuring improved material performance and reduced environmental impact.

2 REVIEW OF CURRENT LITERATURE

Investigations demonstrate that accelerated carbonation hardening (ACH) improves concrete properties such as compressive strength, durability, and resistance to environmental factors. Compressive strength can be improved by 10 % to 50 %, depending on the mix design and carbonation conditions [7, 8]. ACH also reduces permeability and increases resistance to chloride penetration, sulfate attack, and alkali-silica reactions, contributing to the durability of concrete structures [9].

The mechanisms of ACH involve CO₂ diffusion into the moist concrete matrix, where it reacts with calcium hydroxide to form calcium carbonate, enhancing material strength by filling voids [10]. Additionally, ACH densifies the microstructure, improving resistance to environmental and chemical degradation [11-14].

However, carbonation reduces alkalinity, potentially increasing the susceptibility of steel reinforcement to corrosion. Protective calcium carbonate layers formed during ACH may mitigate this risk [15]. The long-term effectiveness

of ACH depends on exposure conditions and material composition, highlighting the need for further performance studies [16].

3 PURPOSE AND METHODOLOGY

The primary objective of this study is to analyze the influence of recipe and technological factors—such as binder content, plasticizer concentration, ground limestone proportions, carbonation pressure, and duration—on the compressive strength of lightweight aggregate concrete at various curing stages (1 hour, 28 days, and 180 days). The goal is to develop experimental-statistical (ES) models that enable the optimization of these factors, ensuring maximum strength while balancing practical and economic constraints.

The research employs experimental design principles, including response surface methodology and desirability functions, to model and optimize material properties. Historical experimental data were analyzed using Design Expert software, allowing for a detailed evaluation of factor interactions and their contributions to strength development. This methodology ensures a comprehensive understanding of the processes governing accelerated carbonation hardening and provides guidance for achieving optimal material performance under varying conditions.

4 RESEARCH RESULTS

Accelerated carbonation hardening (ACH) of lightweight aggregate concrete enhances the carbonation of hydrated cement phases, resulting in the precipitation of calcium carbonates that improve the mechanical properties of the concrete matrix. The ACH process consists of several key stages: surface preparation by cleaning the concrete to ensure uniform CO₂ penetration; installation of specialized carbonation equipment, such as chambers or injection systems; and control of environmental parameters such as temperature and humidity to maximize the reaction kinetics. CO₂ is injected into the concrete through surface holes or internal channels, with continuous monitoring and adjustment of parameters such as CO₂ pressure, temperature, and exposure duration. After the process, the results are

evaluated based on mechanical properties, structure, and carbonation degree.

The rapid development of high early strength within 30 to 60 minutes necessitates carbonation regimes employing elevated pressure. In accordance with the theory of heat and mass transfer, vacuuming freshly molded concrete creates a porous system under reduced pressure. Introducing CO₂ under pressure during this phase accelerates the carbonation process by promoting self-absorption and stress relaxation within the capillary structure. The dissolution rate of minerals increases proportionally with CO₂ pressure, facilitating controlled structure formation.

Earlier investigations identified [2] the optimal aggregate packing for lightweight concrete, with a binder dosage of 300 kg/m³. Concrete strength, density, and other characteristics are influenced by the proportion of fine aggregate particles with a size up to 5 mm. The structure and strength characteristics of carbonized concrete are influenced by three primary factors: the aggregate structure, determined by the distribution of porous aggregate; the binder concentration, defined by cement type and properties; and the mixing water content, adjusted for carbonation technology.

Due to the interaction of recipe and technological factors, the properties of concrete can vary significantly during carbonation. Structure formation is influenced by both constructive and destructive factors, which impact the speed and completeness of reactions. Therefore, optimizing ACH requires analyzing the influence of these factors on early and long-term strength [17]. The optimization criterion focuses on minimizing cement consumption while achieving the required properties, as cement is an expensive and limited resource.

The key recipe-technological factors affecting the physical and mechanical properties of ACH lightweight aggregate concrete include binder consumption, which varies from 300 to 500 kg/m³, with ground limestone content ranging from 0 to 30 %; the plasticizing additive (SYM) content, adjusted between 0 and 0.4 % by binder weight; carbonation pressure, ranging from 0.6 to 1.2 MPa; and the duration of carbonation, set between 30 and 60 minutes.

To develop mathematical models for compressive strength at 1 hour (R_{1h}), 28 days (R_{28}), and 180 days (R_{180}), a second-order five-factor experimental design ("Hartley-5") with six center points was used [18]. The factor levels and variations are presented in Tab. 1.

Table 1 Experimental factors and their ranges of variation

Factors	Quantity unit	Code	Variation levels		
			-1	0	1
A Binder	kg/m ³	<i>Knitt</i>	300	400	500
B SYM additive	%	<i>SYM</i>	0	0.2	0.4
C Ground limestone	%	<i>GL</i>	0	15	30
D Applied carbonation pressure	MPa	P_{CO_2}	0.6	0.9	1.2
E The duration of the carbonization process	min	t_{CO_2}	30	45	60

The study was conducted on cubic samples with an edge length of 10 cm. The molded specimens underwent carbonation under specified conditions. Concrete density,

CO₂ uptake (determined by the weight change of the samples before and after carbonation), and compressive strength were evaluated at specified intervals during the testing process.

The compressive strength of the concrete increased over time, ranging from 2.1 to 16.5 MPa at 1 hour, 4.6 to 21.8 MPa at 28 days, and 5.9 to 26.1 MPa at 180 days. The collected data enabled the creation of experimental-statistical (EC) models for the composite material properties using the Design Expert software [19]. This software allows importing previously obtained experimental data, referred to as "historical" data. The response surface methodology was applied for data analysis. The resulting models and their statistical parameters are presented in Tab. 2. Statistically significant components of the models were selected through backward elimination.

Table 2 EC strength models of material characteristics

Characteristics	Experimental-statistical models for R	Regression Statistics
R_{1h} , MPa	$R_{1h} = +8.80 + 3.70A + 0.90B - 0.50C + 1.30D + 0.50E + 0.40AB + 0.20AD + 0.20AE + 0.40BC - 0.10BD + 0.10BE - 0.30CD - 0.30CE + 0.20DE + 0.98A^2 - 0.52C^2 - 0.52D^2 - 0.32E^2$	$R^2 = 0.9983$ $Adj R^2 = 0.9960$ $Preq R^2 = 0.9979$ $Adeq Precision = 93.028$
R_{28} , MPa	$R_{28} = +12.69 + 5.88A + 1.12B - 1.22C - 0.22D + 0.12E + 0.47AB - 0.28AC - 0.18AD + 0.47BC - 0.13BD + 0.27DE + 1.36A^2 - 0.44B^2 - 0.64C^2 - 0.54E^2$	$R^2 = 0.9984$ $Adj R^2 = 0.9967$ $Preq R^2 = 0.9928$ $Adeq Precision = 90.276$
R_{180} , MPa	$R_{180} = +13.87 + 6.80A + 1.10B - 1.30C - 0.40D + 0.10E + 0.30AB - 0.50AC - 0.20AD - 0.30AE + 0.30BC + 0.30BD + 2.13A^2 - 0.97B^2$	$R^2 = 0.9985$ $Adj R^2 = 0.9973$ $Preq R^2 = 0.9922$ $Adeq Precision = 106.701$

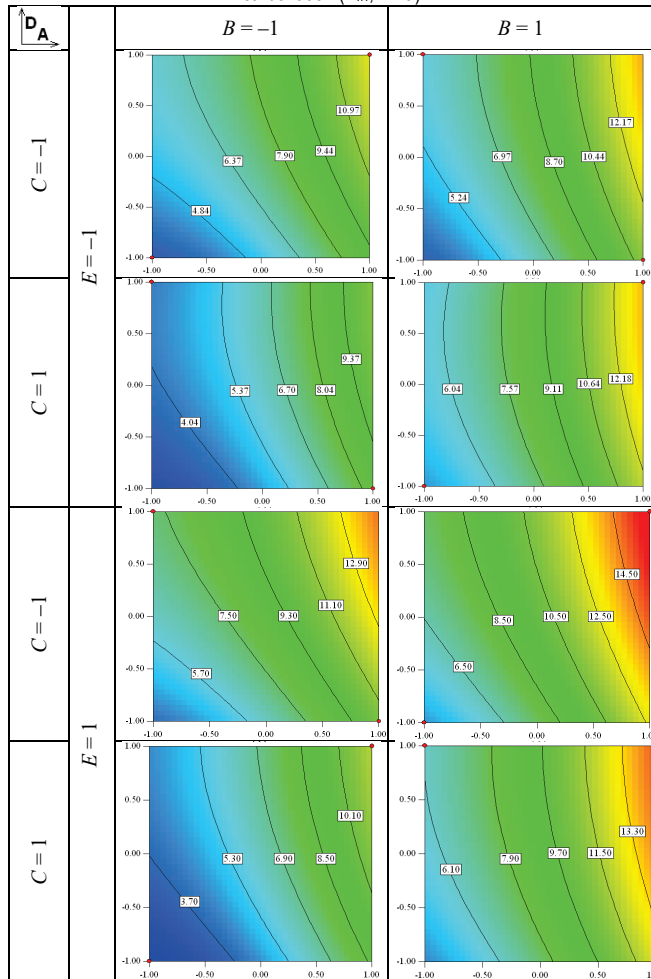
All models exhibited statistical significance. The predicted R^2 values closely matched the adjusted R^2 values, demonstrating consistency. Additionally, the signal-to-noise ratio exceeds the threshold of 4, confirming the reliability of the models. High R^2 values highlight the models' ability to accurately represent the data.

Visualizing the material property field directly is challenging due to the model's multidimensional nature. However, its geometric characteristics can be inferred through line diagrams illustrating the target property (R_{1h} strength in MPa). These diagrams are plotted using two primary factors, A and D , while keeping the other factors (B , C , and E) constant. Since the model shows low sensitivity to changes in B , C , and E , it is practical to analyze isoline maps at the corners of the factorial subspace defined by these three factors. This approach results in eight sections, as detailed in Tab. 3.

As the strength values constitute a time series, a systematic interpretation necessitates a comprehensive analysis of all data, encompassing both analytical and graphical representations. Limestone content (GL , C) follows with a notable negative slope. Factors B , D , and E show less pronounced effects on strength. The model's graphical representation uses isoline maps, where A and C are the primary axes due to their significant influence. Factors B , D , and E , with minimal impact on R_{28} , are presented as discrete

variables. Similar to the analysis for R_{1h} , these factors are positioned at the vertices of the factorial subspace BDE . The corresponding isoline diagrams are provided in Tab. 4.

Table 3 Visual representation of the material's strength field 1hour post-carbonation (R_{1h} , MPa)



Limestone content (GL, C) stands out due to its negative contribution, as shown by the slope at the central point of the plan. Factors B, D , and E are treated as discrete variables, while the primary axes for the graphical analysis remain A and C .

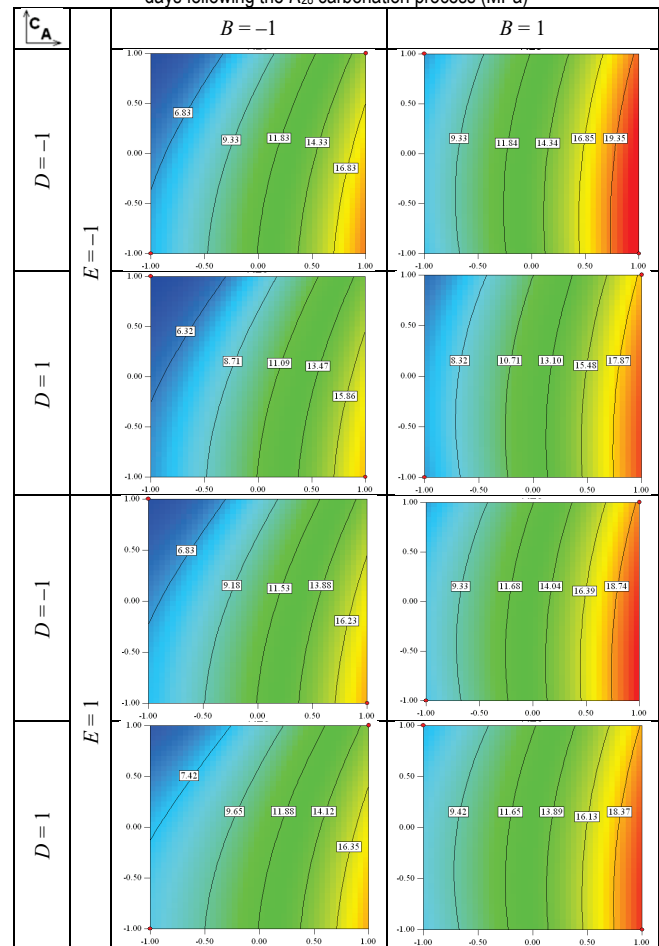
The diagram structure and interpretation approach follow a pattern similar to that in Tab. 3.

The presented mathematical models can be interpreted both from formal mathematical positions and based on the basic concepts of materials science.

There are two main patterns of change in regression models describing the properties over time, provided that they are statistically correctly reduced. During the first stage of development of material structure formation, some of the model components can be split off as insignificant, and at the next stage such components reappear in the models. The second variant observed in the study is associated with stepwise simplification. The terms split off at the first stage do not appear at the subsequent ones. The two variants under consideration are closely related to the existence of "hidden"

parameters of the structure that do not directly affect the properties and are not reflected in the ES-models. Since the prerequisite for the formation of properties and, in particular, strength, is the structure of the material, the difference in the case of two variants of changes in regression models can be interpreted structurally using parameterization methods and the theory of morphogenetic rearrangements of the material structure. According to the corresponding theory [20], the structure of the material under the influence of physicochemical factors undergoes a sequence of rearrangements associated with the implementation of the structural sensitivity of the material. If there is one stage of structural differentiation with the formation of areas with high and, accordingly, low density of particles and bonds (clusters and interfaces), the relaxation process prevails (approaching a stable structural equilibrium).

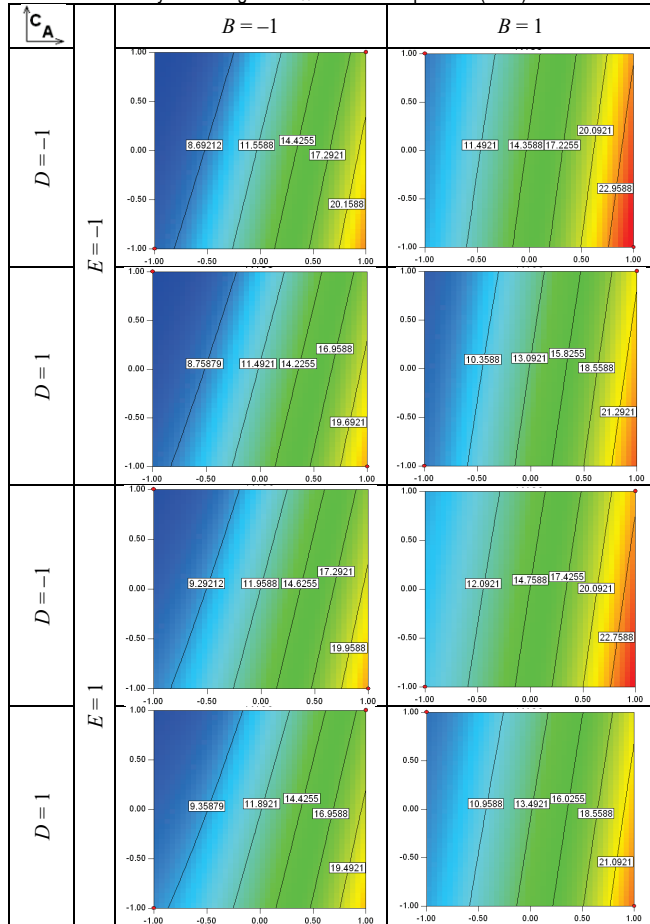
Table 4 Visual representation of the strength distribution within the material 28 days following the R_{28} carbonation process (MPa)



Deviations from this equilibrium decrease, which is associated with a decrease in the influence of a number of structural parameters until they become "hidden". If, however, as a result of the implementation of physicochemical hydration mechanisms, a second phase of sensitivity occurs, associated with dynamic instability, the relaxed characteristics of the structure can again manifest

themselves, affect the properties and, accordingly, enter ES-models. Thus, of the two extreme scenarios, in the material under consideration as a system, the second, relaxation one is realized, with the absence of a repeated stage of sensitivity.

Table 5 Visual representation of the strength distribution within the material 180 days following the R_{180} carbonation process (MPa)



Regression models for strength evolution simplify as hardening progresses. Factors influencing early strength (R_{1h}) diminish in importance over time, with many statistically insignificant terms eliminated by 180 days (R_{180}). This reflects a relaxation process, where structural potential minimizes and linear factor interactions dominate. Thus, the nature of the step-by-step change in regression models can have a phenomenological interpretation from the standpoint of the theory of structure formation.

The influence of binder consumption (A) on strength changes significantly across carbonation stages. At 1 hour, strength increases by 3.2 MPa as levels of SYM additive (B), carbonation pressure (D), and duration (E) rise. Maximum strength is observed at high SYM levels and optimal carbonation parameters. Conversely, at 28 and 180 days, strength growth peaks with high SYM content, no ground limestone (GL , C), and lower pressure and duration values. The relationship between binder consumption and strength follows a second-order function: increasing binder from 300 to 400 kg/m³ boosts strength by 2.7 MPa at 1 hour, 4.2 MPa at 28 days, and 4.5 MPa at 180 days. Ground limestone

content exhibits a dual influence on 1-hour strength. In the absence of SYM , higher contents are detrimental (3.0 MPa reduction), whereas they prove beneficial (1.0 MPa increase) when SYM is incorporated. Over time, limestone's impact diminishes, with binder content and SYM additive becoming dominant. At higher binder levels (500 kg/m³) without SYM , increased limestone reduces strength by 4.0 MPa at 28 days and 4.1 MPa at 180 days. However, with lower binder levels (300 kg/m³) and SYM at 0.4%, replacing cement with limestone up to 30% has negligible effects.

5 OPTIMIZATION OF MATERIAL PROPERTIES

The optimization of recipe-technological factors in this study focuses on three key strength metrics: R_{1h} , R_{28} , and R_{180} . This approach involves multi-criteria optimization, where solutions are derived through compromise to balance competing objectives. A common strategy in such cases is to combine multiple criteria into a single objective function using a convolution method. This method is implemented through desirability functions [21], a tool that facilitates interaction with decision-makers.

The desirability function works by transforming each response or output variable into a dimensionless desirability value, ranging from 0 (completely undesirable) to 1 (fully desirable). These transformed values represent how well each response meets its target or falls within acceptable limits. Once each response is assigned a desirability value, a combined overall desirability score D is calculated as the geometric mean of the individual desirability values (1):

$$D = \left(d_1^{r_1}, d_2^{r_2}, \dots, d_n^{r_n} \right)^{\frac{1}{\sum_i r_i}} \quad (1)$$

where d_i expresses the desirability of each partial criterion, $0 \leq d_i \leq 1$ and r_i expresses its importance.

The Design Expert software was employed for effective multi-criteria optimization and the identification of optimal solutions. Each criterion's importance is rated on a scale from 1 (least important) to 5 (most critical), ensuring a structured and transparent decision-making process.

For the constructed ES-models (Tab. 2), numerous optimization scenarios can be defined, each varying by the assigned importance and weight of criteria. Two scenarios of direct engineering relevance are analyzed further.

The primary objective in developing the composite material is to maximize strength throughout the 180-day hardening period. However, achieving sufficient strength by the standard control point of 28 days is equally critical. To focus on these goals, all additional constraints, aside from those related to fixed intervals, are removed. Under these conditions, partial optimization criteria are established, enabling the formulation of a desirability function that reflects the relative importance of each strength metric. This structured approach ensures the prioritization of long-term performance while maintaining compliance with intermediate benchmarks (Tab. 6).

Table 6 Desirability function parameters for long-term hardening optimization

Factors/properties	Goals	Lower boundary	Upper boundary	Lower weight	Upper weight	Significance
<i>Knitt</i>	within the interval	-1	1	1	1	1
<i>SYM</i>		-1	1	1	1	1
<i>GL</i>		-1	1	1	1	1
<i>P_{CO2}</i>		-1	1	1	1	1
<i>t_{CO2}</i>		-1	1	1	1	1
<i>R_{1h}</i>	maximum	2.1	16.5	1	1	2
<i>R₂₈</i>		3.8	21.8	1	1	2
<i>R₁₈₀</i>		5.9	26.1	1	1	5

As a result of the implementation of the desirability function method, the following solutions were obtained (Tab. 7).

Table 7 Long-term hardening optimization results

No	<i>Knitt</i>	<i>SYM</i>	<i>GL</i>	<i>P_{CO2}</i>	<i>t_{CO2}</i>	<i>R_{1h}</i>	<i>R₂₈</i>	<i>R₁₈₀</i>	<i>Desirability</i>
1	1	0.89	-1	0.08	0.52	14.88	21.21	24.63	0.9268
2	1	0.93	-0.99	0.06	0.51	14.87	21.23	24.60	0.9265
3	1	0.99	-0.98	0	0.54	14.84	21.25	24.60	0.9262
4	1	0.98	-1	-0.17	0.23	14.25	21.48	24.84	0.9257

The selected composition is the optimal solution to the problem under consideration. Its composition and properties are displayed graphically (Fig. 1).

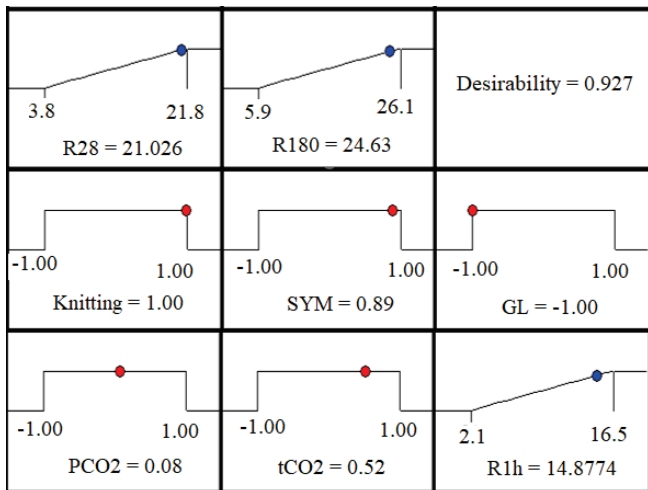


Figure 1 The primary outcome of the multi-criteria optimization of long-term hardening

The composite material optimization focused on minimizing cement consumption and using low-pressure, short-duration carbonation to reduce costs and improve safety. While ensuring the material meets standard strength requirements at 28 days, the primary objective remained maximizing long-term strength. This optimization involved setting partial criteria and assigning importance levels for the desirability function, as shown in Tab. 8.

The following solutions were obtained (Tab. 9).

The corresponding basic solution is reflected in the arch diagram (Fig. 2).

The comparison of Tabs. 8 and 9 reveals that incorporating additional constraints allowed for a more efficient carbonation process and reduced cement usage, albeit with a 6 MPa decrease in long-term strength. The lower desirability values in Tab. 9 highlight the impact of these new

limitations and the need to balance conflicting optimization criteria.

Table 8 Desirability function parameters for long-term hardening optimization, with additional conditions

Factors/properties	Goals	Lower boundary	Upper boundary	Lower weight	Upper weight	Significance
<i>Knitt</i>	within the interval	-1	1	1	1	4
<i>SYM</i>		-1	1	1	1	3
<i>GL</i>		-1	1	1	1	3
<i>P_{CO2}</i>		-1	1	1	1	2
<i>t_{CO2}</i>		-1	1	1	1	2
<i>R_{1h}</i>	maximum	2.1	16.5	1	1	4
<i>R₂₈</i>		3.8	21.8	1	1	5
<i>R₁₈₀</i>		5.9	26.1	1	1	5

Table 9 Optimization results for long-term hardening under constraints

No	<i>Knitt</i>	<i>SYM</i>	<i>GL</i>	<i>P_{CO2}</i>	<i>t_{CO2}</i>	<i>R_{1h}</i>	<i>R₂₈</i>	<i>R₁₈₀</i>	<i>Desirability</i>
1	0.57	1	-0.49	-1	-1	9.29	17.89	20.23	0.5838
2	0.57	1	-0.48	-1	-1	9.32	17.91	20.24	0.5837
3	0.57	1	-0.48	-1	-0.98	9.33	17.91	20.23	0.5836
4	0.57	1	-0.52	-1	-1	9.28	17.92	20.29	0.5835

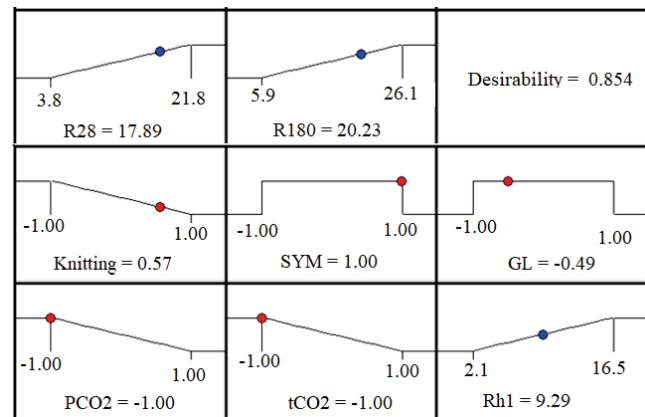


Figure 2 The primary outcome of the multi-criteria optimization of long-term hardening with constraints

6 CONCLUSION

The analysis of strength data for carbonized lightweight aggregate concrete allowed for the development of experimental-statistical models (ES-models) to predict material properties. Compressive strength ranged from 2.1 to 16.5 MPa one hour after carbonation, 4.6 to 21.8 MPa at 28 days, and 5.9 to 26.1 MPa at 180 days. Graphical representations and interpretations of these models support the hypothesis that, as the concrete structure forms, ES-models tend to simplify by removing interactions between structural factors. Two optimization tasks were formulated: the first focused on maximizing long-term strength without additional constraints, while the second incorporated limits on cement usage and carbonation parameters. The desirability function approach determined optimal factor sets. For the second task, the optimal mix included *Knitt* = 0.57, *SYM* = 1, *GL* = -0.49, and *P_{CO2}* = -1, yielding strengths of 9.29 MPa (1 hour), 17.89 MPa (28 days), and 20.23 MPa (180 days). These constraints achieved cement savings and optimized carbonation conditions, though long-term strength decreased by about 6 MPa.

Acknowledgments

This work has been supported by Metal Centre Čakovec under the project KK.01.1.1.02.0023

7 REFERENCES

- [1] Teir, S., Eloneva, S. & Zevenhoven, R. (2005). Production of precipitated calcium carbonate from calcium silicates and carbon dioxide. *Energy Conversion and Management*, 46, 2954-2979. <https://doi.org/10.1016/j.enconman.2005.02.009>
- [2] Groves, G., Rodway, D. & Richardson, I. (1990). The carbonation of hardened cement pastes. *Advances in Cement Research*, 3(11), 117-125. <https://doi.org/10.1680/adcr.1990.3.11.117>
- [3] Gara, O. A., Kolesnykov, A. V., Semenova, S. V. & Oliinyk T. P. (2024) Optimization of accelerated carbonation hardening effects of expanded clay concrete, *Modern construction and architecture*, 8, 50-64. <https://doi.org/10.31650/2786-6696-2024-8-50-64>
- [4] Kashef-Haghighi, S. & Ghoshal, S. (2013). Physico-chemical processes limiting CO₂ uptake in concrete during accelerated carbonation curing. *Industrial & Engineering Chemistry Research*, 52(16), 5529-5537. <https://doi.org/10.1021/ie303372h>
- [5] Suescum-Morales, D., Kalinowska-Wichrowska, K., Fernández, J. M. & Jimenez, J. R. (2021). Accelerated carbonation of fresh cement-based products containing recycled masonry aggregates for CO₂ sequestration. *Journal of CO₂ Utilization*, 46, 101461. <https://doi.org/10.1016/j.jcou.2021.101461>
- [6] Gara, O. A. (2016). Features of Carbonation Hardening of Lightweight Aggregate Concrete. *Visnjik ODABA*, 62, 22-27. (in Ukrainian)
- [7] Rostami, V., Shao, Y., Boyd, A. J. & He, Z. (2012). Microstructure of cement paste subject to early carbonation curing. *Cement and Concrete Research*, 42(1), 186-193. <https://doi.org/10.1016/j.cemconres.2011.09.003>
- [8] Lagerblad, B. (2005). Carbon dioxide uptake during concrete life cycle - State of the art. Swedish Cement and Concrete Research Institute.
- [8] Junior, A., Filho, R., Fairbairn, E. & Dweck, J. (2014). A study of the carbonation profile of cement pastes by thermogravimetry and its effect on the compressive strength. *Journal of Thermal Analysis and Calorimetry*, 116, 69-76. <https://doi.org/10.1007/s10973-014-3922-9>
- [10] Šavija, B. & Luković, M. (2016). Carbonation of cement paste: Understanding, challenges, and opportunities. *Construction and Building Materials*, 117, 285-301. <https://doi.org/10.1016/j.conbuildmat.2016.04.138>
- [11] Parrott, L. (1992). Carbonation, moisture and empty pores. *Advances in Cement Research*, 4(15), 111-118. <https://doi.org/10.1680/adcr.1992.4.15.111>
- [12] Shi, C., Tu, Z., Guo, M. Z. & Wang, D. (2017). Accelerated carbonation as a fast curing technology for concrete blocks. In *Sustainable and Nonconventional Construction Materials Using Inorganic Bonded Fiber Composites* (pp. 313-341). Woodhead Publishing. <https://doi.org/10.1016/B978-0-08-102001-2.00014-0>
- [13] Thiery, M., Villain, G., Dangla, P. & Platret, G. (2007). Investigation of the carbonation front shape on cementitious materials: Effects of the chemical kinetics. *Cement and Concrete Research*, 37(7), 1047-1058. <https://doi.org/10.1016/j.cemconres.2007.04.002>
- [14] Morandeau, A., Thiery, M. & Dangla, P. (2014). Investigation of the carbonation mechanism of CH and CSH in terms of kinetics, microstructure changes and moisture properties. *Cement and Concrete Research*, 56, 153-170. <https://doi.org/10.1016/j.cemconres.2013.11.015>
- [15] Bertolini, L., Elsener, B., Pedeferri, P., Redaelli, E. & Polder, R. B. (2013). *Corrosion of Steel in Concrete: Prevention, Diagnosis, Repair*. John Wiley & Sons. <https://doi.org/10.1002/9783527651696>
- [16] Matthews, J. (1984). Carbonation of ten-year-old concretes with and without PFA. *Proceedings of AshTech*.
- [17] Gara, A. A. (1990). Development of Carbonation Technology for Lightweight Aggregate Concrete Wall Products. *Doctoral dissertation*. Odesskij inženerno-stroitel'nij institut. (in Ukrainian)
- [18] Adler, Y. P., Markova, E. V. & Granovskiy, Y. V. (1976). Experiment Planning for Finding Optimal Conditions. (in Russian)
- [19] Grant, F. (2007). *Design Expert 7.1*. Scientific Computing World.
- [20] Kolesnikov, A. V., Semenova, S. V. & Makovetska, O. O. (2023). Modeling of Composite Structure Formation Processes Using Catastrophe Theory. *Sucasne budivnictvo ta arhitektura*, 6, 90-98. (in Ukrainian)
- [21] Myers, R. H., Montgomery, D. C. & Anderson-Cook, C. M. (2009). *Response Surface Methodology: Process and Product Optimization Using Designed Experiments*. John Wiley & Sons. <https://doi.org/10.1002/9780470744581>

Authors' contacts:

Olexander Gara, PhD, Assistant Professor
Odessa State Academy of Civil Engineering and Architecture,
Construction and Technological Institute,
Department of Processes and Apparatuses in the Technology of Building Materials,
Didrihsona st., 4, 65029 Odesa, Ukraine
garaogasa@ukr.net

Anatolij Gara, PhD, Assistant Professor
Odessa State Academy of Civil Engineering and Architecture,
Construction and Technological Institute,
Department of Production of Construction Products and Structures,
Didrihsona st., 4, 65029 Odesa, Ukraine
ggaryc223420@gmail.com

Andrii Kolesnykov, PhD, Assistant Professor
Odessa State Academy of Civil Engineering and Architecture,
Construction and Technological Institute,
Department of Chemistry and Ecology,
Didrihsona st., 4, 65029 Odesa, Ukraine
Kolesnikov_himek@odaba.edu.ua

Khrystyna Moskalova, PhD, Assistant Professor
(Corresponding author)
Development and Training Centre for the Metal Industry—Metal Centre Čakovec,
Department for Research and Development,
Bana Josipa Jelačića, 22D, 40000 Čakovec, Croatia
kristina@metalskajezgra.hr